Thermochimica Acta 499 (2010) 106–110

Contents lists available at ScienceDirect

Thermochimica Acta

journal homepage: www.elsevier.com/locate/tca

Elimination behavior of nitrogen oxides from a NO_3^--intercalated Mg–Al layered double hydroxide during thermal decomposition

Tomohito Kameda*, Yuki Fubasami, Naoya Uchiyama, Toshiaki Yoshioka

Graduate School of Environmental Studies, Tohoku University, 6-6-07 Aoba, Aramaki, Aoba-ku, Sendai 980-8579, Japan

ARTICLE INFO

Article history:
Received 19 August 2009
Received in revised form
11 November 2009
Accepted 17 November 2009
Available online 24 November 2009

Keywords:
Elimination
Nitrogen oxides
Mg–Al layered double hydroxide
Thermal decomposition
TG–MS

ABSTRACT

The thermal properties of NO_3^--intercalated Mg–Al layered double hydroxide (NO_3·Mg–Al LDH) were investigated using simultaneous thermogravimetry–mass spectrometry (TG–MS), and the elimination behavior of nitrogen oxides from this double hydroxide was examined. The TG–MS results showed that NO_3·Mg–Al LDH decomposed in four stages. The first stage involved evaporation of surface adsorbed water and interlayer water in NO_3·Mg–Al LDH. In the second and third stages, dehydroxylation of the brucite-like octahedral layers in NO_3·Mg–Al LDH occurred. The fourth stage mainly corresponded to the elimination of NO_3^- intercalated in the Mg–Al LDH interlayers to afford NO_2. Thermal decomposition of NO_3·Mg–Al LDH at 400–600 °C resulted in the formation of Mg–Al oxide, and the produced NO_2 reacted with H_2O and O_2 to form HNO_3 and HNO_2. The elimination of nitrogen oxides was found to increase with time and decomposition temperature. The synthesized Mg–Al oxide mixture could be used to remove nitric acid from aqueous solutions.

1. Introduction

It has been found that Mg–Al layered double hydroxide (Mg–Al LDH) can be used as an adsorbent for the removal of anionic pollutants in aqueous media [1–8]. Mg–Al LDH can be used as an anion exchanger [9] and is represented by the formula $[Mg^{2+}_{1-x}Al^{3+}_x(OH)_2](A^{n-})_{x/n}\cdot mH_2O$, where A^{n-} is an anion such as CO_3^{2-} and Cl^-, and x is the Al/(Mg + Al) molar ratio ($0.20 \leqq x \leqq 0.33$) [10,11]. Mg–Al LDH consists of brucite-like octahedral layers that are positively charged because of the replacement of some Mg^{2+} units by Al^{3+}, while the interlayer anions help in maintaining charge balance. Water (H_2O) molecules occupy the remaining spaces in the interlayer. CO_3^{2-}-intercalated Mg–Al LDH (CO_3·Mg–Al LDH) can be converted to Mg–Al oxide by calcination at 450–800 °C. The formation of Mg–Al oxide is represented by the following reaction:

$$Mg_{1-x}Al_x(OH)_2(CO_3)_{x/2} \rightarrow Mg_{1-x}Al_xO_{1+x/2} + (x/2)CO_2 + H_2O \quad (1)$$

The resulting Mg–Al oxide undergoes rehydration and combines with anions to afford the original LDH structure, as shown in the following equation:

$$Mg_{1-x}Al_xO_{1+x/2} + x/nA^{n-} + (1+x/2)H_2O \rightarrow Mg_{1-x}Al_x(OH)_2A_{x/n} + xOH^- \quad (2)$$

The abovementioned rehydration and subsequent combination of Mg–Al oxide with anions in solution are accompanied by the release of OH^-. Accordingly, Mg–Al oxide can neutralize and fix NO_3^- when used in the treatment of HNO_3 [12]. Subsequently, NO_3^--intercalated Mg–Al LDH (NO_3·Mg–Al LDH) is produced by the reconstruction of Mg–Al oxide. In actual wastewater treatment, large quantities of Mg–Al oxide are used, and hence, considerable amounts of waste NO_3·Mg–Al LDH are generated. If Mg–Al oxide can be regenerated from the obtained NO_3·Mg–Al LDH and reused to treat waste HNO_3, the energy required for the synthesis of Mg–Al oxide and CO_3·Mg–Al LDH will be drastically reduced, and the formation of NO_3·Mg–Al LDH wastes can be prevented. In order to effectively reuse Mg–Al oxide for the treatment of HNO_3, it is necessary to examine in detail the thermal decomposition behavior of NO_3·Mg–Al LDH and the elimination of nitrogen oxides.

In this study, we investigated the thermal properties of NO_3·Mg–Al LDH by simultaneous thermogravimetry–mass spectrometry (TG–MS). In addition, we carried out thermal decomposition of NO_3·Mg–Al LDH in air and investigated the effect of temperature on its elimination behavior of nitrogen oxides. We also examined the capability for the treatment of HNO_3 with Mg–Al oxides obtained by the thermal decomposition of NO_3·Mg–Al LDHs at different temperature.

2. Experimental

2.1. Preparation

NO_3·Mg–Al LDH was prepared by the co-precipitation method. The Mg–Al solution (0.4 M $Mg(NO_3)_2$ + 0.1 M $Al(NO_3)_3$) was pre-

* Corresponding author. Tel.: +81 22 795 7212; fax: +81 22 795 7212.
E-mail address: kameda@env.che.tohoku.ac.jp (T. Kameda).

0040-6031/$ – see front matter © 2009 Elsevier B.V. All rights reserved.
doi:10.1016/j.tca.2009.11.009

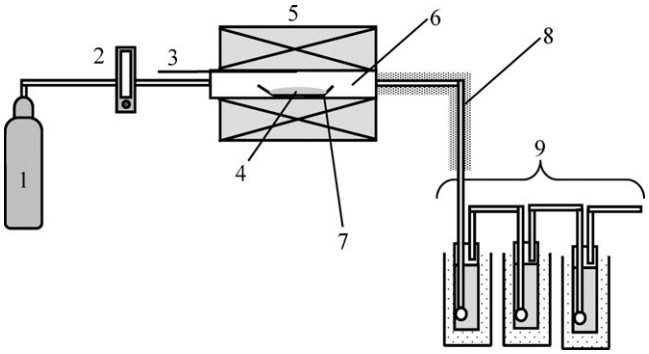

Fig. 1. Experimental apparatus used for thermal decomposition of NO_3·Mg–Al LDH. (1) Air cylinder; (2) flow meter; (3) thermocouple; (4) sample; (5) electric furnace; (6) quartz reaction tube; (7) aluminum boat; (8) flexible heater; and (9) water trap (0 °C).

pared by dissolving $Mg(NO_3)_2{\cdot}6H_2O$ (0.1 mol) and $Al(NO_3)_3{\cdot}9H_2O$ (0.025 mol) in 250 mL of deionized water. The Mg–Al solution was added dropwise to 250 mL of 0.3 mM NaOH solution at 30 °C with mild agitation. The solution pH was adjusted to 10.5 by adding 0.5 M NaOH solution. The mixture was then stirred continuously at 30 °C for 1 h. The NO_3·Mg–Al LDH that formed was isolated by filtering the resulting suspension, washing it thoroughly with deionized water, and drying it under reduced pressure (133 Pa) at 40 °C for 40 h. The NO_3·Mg–Al LDH crystals were ground into powder using a mortar and pestle, and the resulting powder was characterized by X-ray diffraction (XRD) using a Rigaku RINT-2200VHF diffractometer (Rigaku Corp., Tokyo, Japan) with CuKα radiation at 40 kV and 20 mA (scan rate: 2° min^{-1}). The NO_3·Mg–Al LDH was dissolved in 1 M HNO_3, and analyzed for Mg^{2+} and Al^{3+} using inductively coupled plasma–atomic emission spectrometry (ICP–AES). The NO_3·Mg–Al LDH was also dissolved in 0.1 M HCl, and analyzed for NO_3^- using a Dionex DX-120 ion chromatograph equipped with an AS-12A column (eluent: 2.7 mM Na_2CO_3 and 0.3 mM $NaHCO_3$; flow rate: 1.3 mL min^{-1}).

2.2. Thermal properties of NO_3·Mg–Al LDH

A 10-mg sample of NO_3·Mg–Al LDH was analyzed by simultaneous TG (Seiko Instruments TG/DTA 6200) and MS (Hewlett Packard 5973) at a heating rate of 5 °C min^{-1} in a He flow rate of 200 mL min^{-1}. The decomposition products were introduced to the MS ion source through an inactivated stainless steel capillary tube heated at 300 °C to prevent condensation of the evolved products.

2.3. Elimination behavior of nitrogen oxides from NO_3·Mg–Al LDH

The experimental apparatus used for carrying out the thermal decomposition of NO_3·Mg–Al LDH is shown in Fig. 1. An aluminum boat containing 0.5 g of NO_3·Mg–Al LDH was inserted in a quartz reaction tube, which was placed in an electric furnace. NO_3·Mg–Al LDH decomposed at 400–600 °C at an air flow rate of 50 mL min^{-1}. The evolved gas was collected in three water traps (0 °C) containing 30 mL deionized water. In order to prevent condensation of the evolved gas, the line from the quartz reaction tube to the trap was heated to 110–130 °C using a flexible heater. The anions in the traps were quantified using ion chromatograph. The products obtained in the thermal decomposition of NO_3·Mg–Al LDH were identified by XRD analysis.

2.4. Treatment of HNO_3

Mg–Al oxides, obtained by the thermal decomposition of NO_3·Mg–Al LDH at 400–600 °C using the experimental apparatus shown in Fig. 1, were examined to check the capability for the treatment of HNO_3. 10 mL of 0.1 M HNO_3 solution were added to a pre-determined amount of $Mg_{0.80}Al_{0.20}O_{1.10}$ in 50-mL screw-top tubes, and shaken at 25 °C for 24 h. The quantity of $Mg_{0.80}Al_{0.20}O_{1.10}$ used was a stoichiometric quantity according to Eq. (3).

$$Mg_{0.80}Al_{0.20}O_{1.10} + 0.20HNO_3 + 0.90H_2O \rightarrow Mg_{0.80}Al_{0.20}(OH)_2(NO_3)_{0.20} \quad (3)$$

The NO_3^- concentration of the filtrate was determined using the ion chromatograph.

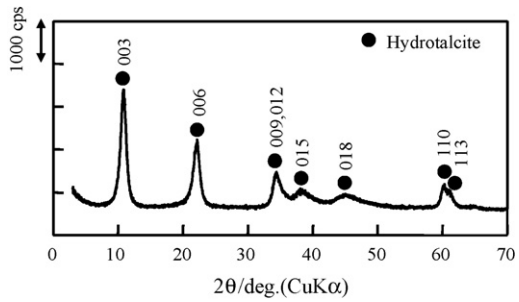

Fig. 2. XRD patterns for NO_3·Mg–Al LDH.

3. Results and discussion

3.1. Preparation

The XRD patterns obtained for NO_3·Mg–Al LDH (Fig. 2) are ascribed to hydrotalcite (JCPDS card 22-700), a naturally occurring hydroxycarbonate of magnesium and aluminum ($Mg_6Al_2(OH)_{16}CO_3{\cdot}4H_2O$), and show that NO_3·Mg–Al LDH has an LDH structure. Table 1 lists the chemical composition of NO_3·Mg–Al LDH. The molar ratios of Mg/Al and NO_3/Al are 3.9 and 0.83, respectively. The Mg/Al molar ratio is similar to the expected value for the preparation procedure in this study. The NO_3/Al molar ratio is 83% of the expected value, which is calculated from the neutralization of the positive charge of the Al-bearing brucite-like octahedral layers. This suggests that the NO_3^- content in NO_3·Mg–Al LDH is governed by the charge balance in Mg–Al LDH. Accordingly, NO_3^--intercalated Mg–Al LDH was confirmed to be prepared by the co-precipitation method.

3.2. Thermal properties of NO_3·Mg–Al LDH

Recently, Frost et al. have aggressively examined the thermal decompositions of many kinds of LDHs such as CO_3·Mg–Al LDH, VO_4·Mg–Al LDH, MoO_4·Mg–Al LDH, AsO_4·Mg–Al LDH, PO_4·Mg–Al LDH, CO_3·Mg–(Fe,Al) LDH, CO_3·Mg–(Fe,Cr) LDH, CO_3·Cu–Al LDH, and CO_3·Zn–Al LDH [13–18]. Frost's review presents that the thermal decomposition of CO_3·Mg–Al LDH, which is the representative LDH, occurs in three steps: (i) removal of adsorbed water, (ii) elimination of the interlayer structural water, and (iii) the simultaneous dehydroxylation and decarbonation of the hydrotalcite framework [19]. Compared to these results, thermal properties of NO_3·Mg–Al LDH were analyzed as follows.

Table 1
Chemical composition of NO_3·Mg–Al LDH.

Mass %			Molar ratio	
Mg	Al	NO_3	Mg/Al	NO_3/Al
23.7	6.7	12.7	3.9	0.83

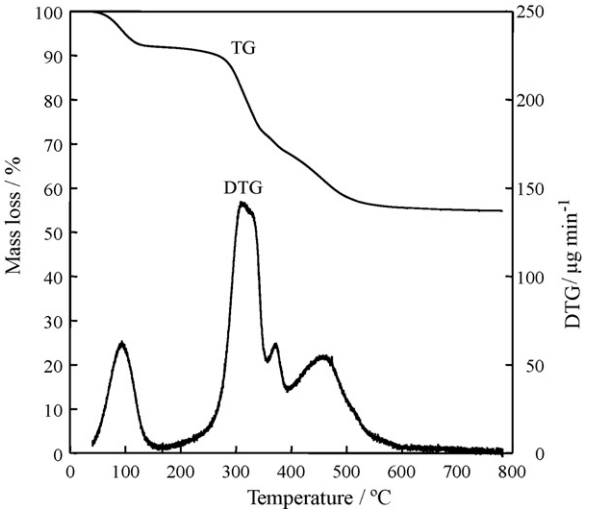

Fig. 3. TG and DTG curves for NO_3·Mg–Al LDH.

Fig. 3 shows the TG and differential thermal gravimetry (DTG) curves obtained for NO_3·Mg–Al LDH. Decomposition of NO_3·Mg–Al LDH occurred in the following four stages: stage 1, mass loss of 0–8% until 120 °C; stage 2, mass loss of 8–26% at 120–350 °C; stage 3, mass loss of 26–31% at 350–380 °C; and stage 4, mass loss of 26–45% above 380 °C. The first stage corresponded to the evaporation of surface adsorbed water and interlayer water in NO_3·Mg–Al LDH. The second and third stages were mainly attributable to the dehydroxylation of the brucite-like octahedral layers in NO_3·Mg–Al LDH. The fourth stage was most probably due to the elimination of NO_3^- intercalated in the Mg–Al LDH interlayers. Fig. 4 shows the TG curves obtained for NO_3·Mg–Al LDH and the mass spectra of selected ions from among the major thermal decomposition products of NO_3·Mg–Al LDH. The mass spectrum showed signals at m/z 18, 30, 32, 44, and 46, which corresponded to the molecular ion peaks of H_2O^+, NO^+, O_2^+, CO_2^+, and NO_2^+, respectively. The H_2O^+ peak in the spectrum showed that H_2O was produced at four steps, i.e., during the elimination of surface adsorbed water and interlayer water (stage 1), dehydroxylation of NO_3·Mg–Al LDH components whose properties were similar to those of $Al(OH)_3$ and $Mg(OH)_2$ (stages 2 and 3, respectively), and dehydroxylation of NO_3·Mg–Al LDH components whose properties were similar to those of $Al(OH)_3$ (stage 4) [20]. The NO^+ and NO_2^+ peaks were

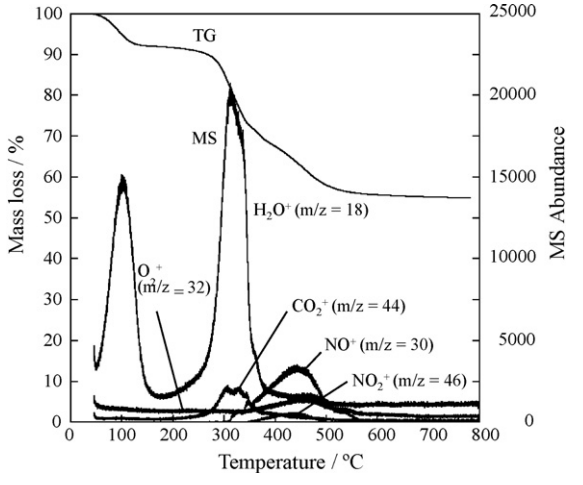

Fig. 4. TG curve of NO_3·Mg–Al LDH and selected-ion mass spectra of major products formed in thermal decomposition of NO_3·Mg–Al LDH.

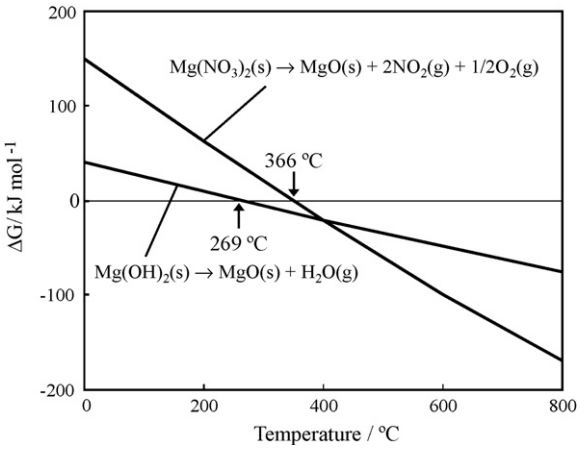

Fig. 5. Gibbs free energy change (ΔG) for the decomposition of $Mg(OH)_2$ and $Mg(NO_3)_2$.

observed at 300–600 °C and 350–500 °C in the mass spectra, respectively (Fig. 4). The intensities of the NO^+ and NO_2^+ peaks were high in the fourth decomposition stage (>380 °C), confirming that the mass loss of NO_3·Mg–Al LDH in this stage was due to the formation of nitrogen oxides by the elimination of intercalated NO_3^-. The NO_2^+ peak definitely corresponds to the occurrence of NO_2. The NO^+ peak generally corresponds to the occurrence of NO and NO_2. However, the NO^+ peak in this study probably suggests the main formation of NO_2, because the evolved nitrogen oxides by the thermal decomposition of $Mg(NO_3)_2$·$6H_2O$ were observed to be only NO_2 in the TG-FTIR spectroscopy despite the presence of the m/z = 30 ion fragment in TG–MS [21]. This is also supported by the fact that the m/z = 30 ion fragment is the most intense fragment of NO_2 gas according to the reference mass spectra in NIST database [22]. Therefore, the elimination of NO_3^- intercalated in the interlayer of NO_3·Mg–Al LDH during the thermal decomposition is certainly caused by the main formation of NO_2. A prominent O_2^+ peak corresponding to the production of O_2 was observed at 400–500 °C. This is probably derived from the decomposition of NO_3^- in NO_3·Mg–Al LDH in the fourth decomposition stage (>380 °C). The decomposition pattern of NO_3·Mg–Al LDH is determined thermodynamically as follows. The thermal properties of NO_3·Mg–Al LDH are assumed to resemble those of $Mg(OH)_2$ and $Mg(NO_3)_2$. Therefore, the Gibbs free energy change (ΔG) for the decomposition of $Mg(OH)_2$ and $Mg(NO_3)_2$ (shown in Eqs. (4) and (5)) is determined using the thermochemical data reported by Binnewies and Milke [23], as shown in Fig. 5:

$$Mg(OH)_2 \rightarrow MgO + H_2O \quad (4)$$

$$Mg(NO_3)_2 \rightarrow MgO + 2NO_2 + (1/2)O_2 \quad (5)$$

In the decomposition of $Mg(OH)_2$ and $Mg(NO_3)_2$, the temperatures corresponding to $\Delta G < 0$ were found to exceed 269 and 366 °C, respectively. This implied that the decomposition of NO_3·Mg–Al LDH was thermodynamically favorable, resulting in the production of H_2O and NO_2. In fact, the temperature for H_2O production from the dehydroxylation of NO_3·Mg–Al LDH was lower than that for NO_2 production (Fig. 4). This result was in good agreement with the thermodynamic consideration that the temperature for $Mg(OH)_2$ decomposition is lower than that for $Mg(NO_3)_2$ decomposition. By the way, a CO_2^+ peak, which corresponded to the formation of CO_2, was observed at 250–400 °C in the mass spectrum (Fig. 4), indicating the elimination of CO_2 from NO_3·Mg–Al LDH. As shown in Table 1, the NO_3/Al molar ratio in the NO_3·Mg–Al LDH was lower than 1.0, suggesting that CO_3^{2-} in addition to NO_3^- was intercalated in the interlayer of Mg–Al LDH in order to compensate the

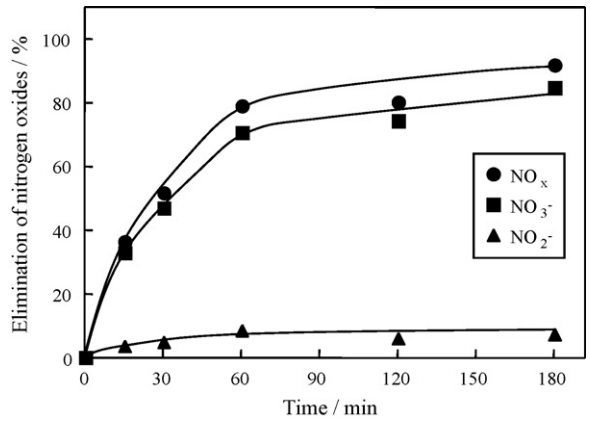

Fig. 6. Variation in the elimination of nitrogen oxides with time in the thermal decomposition of NO_3·Mg–Al LDH at 400 °C.

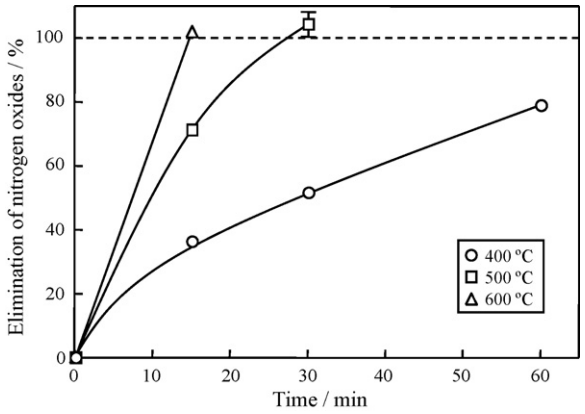

Fig. 7. Effect of temperature on the elimination of nitrogen oxides in the thermal decomposition of NO_3·Mg–Al LDH.

positive charge of the Al-bearing brucite-like octahedral layers. This contamination by CO_3^{2-} is due to the dissolution of CO_2 into the solution in the preparation procedure. The elimination of CO_2 certainly does not affect the production of NO_2. Fig. 4 also presents that CO_2^+ and H_2O^+ peaks were observed at 250–400 °C, respectively, supporting the simultaneous dehydroxylation and decarbonation of the CO_3·Mg–Al LDH, as mentioned by Frost's review [19]. In case of NO_3·Mg–Al LDH, the dehydroxylation and elimination of NO_3^- were found to occur differently, confirmed by the fact that the NO^+ and NO_2^+ peaks were mainly observed at around 400–500 °C in the mass spectra, respectively (Fig. 4).

To summarize, the decomposition of NO_3·Mg–Al LDH proceeded in four stages. Stage 1: evaporation of surface adsorbed water and interlayer water in NO_3·Mg–Al LDH; stages 2 and 3: dehydroxylation of the brucite-like octahedral layers in NO_3·Mg–Al LDH; and stage 4: elimination of NO_3^- intercalated in the Mg–Al LDH interlayers to afford NO_2.

3.3. Elimination behavior of nitrogen oxides from NO_3·Mg–Al LDH

In this section, we report the elimination behavior of nitrogen oxides from NO_3·Mg–Al LDH estimated using the experimental apparatus shown in Fig. 2 and the production of Mg–Al oxide. Fig. 6 shows the variation in the elimination of nitrogen oxides with time during the thermal decomposition of NO_3·Mg–Al LDH at 400 °C. Since NO_2^- and NO_3^- are detected in the water traps, the elimination of nitrogen oxides is expressed as the ratio of the mole percent of NO_2^- and NO_3^- in the traps to that of NO_3^- in NO_3·Mg–Al LDH. The elimination of nitrogen oxides increases with time, reaching 91.7% in 180 min. The solutions in the traps are strongly acidic, thus confirming the production of HNO_3 and HNO_2. The thermal decomposition of NO_3·Mg–Al LDH results in the main formation of NO_2. NO_2 then reacts with H_2O and O_2 to form HNO_3 and HNO_2 in the manner shown in Eqs. (6) and (7), respectively [24,25].

$$2NO_2 + H_2O \rightarrow HNO_3 + HNO_2 \quad (6)$$

$$2NO_2 + H_2O + (1/2)O_2 \rightarrow 2HNO_3 \quad (7)$$

As shown in Fig. 6, the elimination for NO_3^- is considerably higher than that for NO_2^- at any given instant. This indicates that the production of HNO_3 is mainly caused by the reaction shown in Eq. (7).

Fig. 7 shows the effect of temperature on the elimination of nitrogen oxides in the thermal decomposition of NO_3·Mg–Al LDH. At 400 °C, the elimination of nitrogen oxides increased gradually with time, reaching 78.9% in 60 min. At 500 and 600 °C, the elimination of nitrogen oxides increased rapidly with time, reaching 100% within 30 and 15 min, respectively. The elimination of nitrogen oxides was thus confirmed to increase with temperature as well. Notably, all the intercalated NO_3^- was lost from NO_3·Mg–Al LDH at 500 and 600 °C, and this explained why the NO_2^+ and NO^+ peaks could not be detected in the mass spectrum at temperatures above 500 and 600 °C, respectively (Fig. 4). Fig. 8 presents the XRD patterns for the products obtained in the thermal decomposition of NO_3·Mg–Al LDH under different heating conditions. Although the product obtained at 1100 °C after 180 min was a mixture of MgO and $MgAl_2O_4$, only Mg–Al oxide was obtained under other conditions. Thus, it could be confirmed that the thermal decomposition of NO_3·Mg–Al LDH at 400–600 °C results in the formation of Mg–Al oxide only.

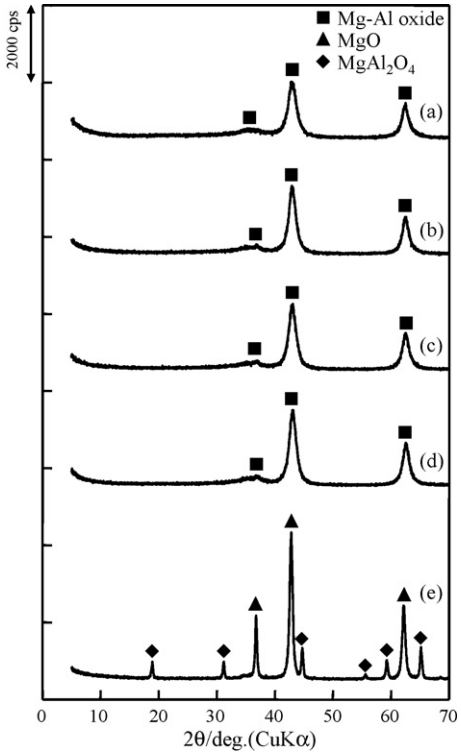

Fig. 8. XRD patterns for products obtained in the thermal decomposition of NO_3·Mg–Al LDH under different heating conditions: (a) 400 °C, 15 min; (b) 500 °C, 15 min; (c) 600 °C, 15 min; (d) 600 °C, 60 min; and (e) 1100 °C, 180 min.

Table 2
Degree of NO_3^- removal from HNO_3 solution by Mg–Al oxides obtained with various temperatures.

Temperature/°C	NO_3^- removal/%
400	52.5
500	78.0
600	65.3

3.4. Treatment of HNO_3

Fig. 7 presents the highest eliminations of nitrogen oxides at 400 °C for 60 min, at 500 °C for 30 min, and at 600 °C for 15 min, respectively. Mg–Al oxides, converted from NO_3·Mg–Al LDHs with these conditions, were examined to treat HNO_3. Table 2 shows the degree of NO_3^- removal from HNO_3 solution by the Mg–Al oxides. All Mg–Al oxides were able to remove NO_3^- from HNO_3 solution. As shown in Fig. 7, some NO_3^- is remained in Mg–Al oxide obtained at 400 °C for 60 min. The remaining of NO_3^- leads to the lowest degree of NO_3^- removal for Mg–Al oxide obtained at 400 °C. The degree of NO_3^- removal for 500 °C was higher than that for 600 °C, although NO_3^- was completely lost in Mg–Al oxides obtained at both temperatures. The high temperature probably promotes the crystallization of Mg–Al oxide for the conversion to MgO and $MgAl_2O_4$. This crystallization likely results in the decrease of NO_3^- removal capability.

4. Conclusions

The thermal decomposition of NO_3·Mg–Al LDH occurred in the following four stages: evaporation of surface adsorbed water and interlayer water (stage 1), dehydroxylation of the brucite-like octahedral layers in NO_3·Mg–Al LDH (stages 2 and 3), and elimination of NO_3^- intercalated in the Mg–Al LDH interlayers to afford NO_2 (stage 4). The thermal properties of NO_3·Mg–Al LDH were considered to be similar to those of $Mg(OH)_2$ and $Mg(NO_3)_2$. The temperature for H_2O formation from the dehydroxylation of NO_3·Mg–Al LDH was lower than that for NO_2 production. This observation was consistent with the thermodynamic consideration that the temperature for $Mg(OH)_2$ decomposition is lower than that for $Mg(NO_3)_2$ decomposition. NO_2, which was produced by the thermal decomposition of NO_3·Mg–Al LDH at 400–600 °C, reacted with H_2O and O_2 to form HNO_3 and HNO_2. The elimination of nitrogen oxides was found to increase with the decomposition time and temperature. Further, all the intercalated NO_3^- was completely eliminated from NO_3·Mg–Al LDH at 500 and 600 °C, confirming that Mg–Al oxide was produced upon the thermal decomposition of NO_3·Mg–Al LDH at 400–600 °C. The Mg–Al oxide was able to treat HNO_3 solution. To summarize, complete loss of nitrogen oxides of NO_3·Mg–Al LDH and formation of Mg–Al oxide occurred in the thermal decomposition of NO_3·Mg–Al LDH. On the basis of the present results, we concluded that cyclic usage of Mg–Al oxide for the treatment of HNO_3 is possible.

References

[1] F. Cavani, F. Trifiro, A. Vaccari, Catal. Today 11 (1991) 173.
[2] S.P. Newman, W. Jones, New J. Chem. 22 (1998) 105.
[3] A.D. Roy, Mol. Cryst. Liq. Cryst. 311 (1998) 173.
[4] Y. You, G.F. Vance, H. Zhao, Appl. Clay Sci. 20 (2001) 13.
[5] M.Z. Hussein, Z. Zainal, I. Yaziz, T.C. Beng, J. Environ. Sci. Health A 36 (2001) 565.
[6] B. Dousova, V. Machovic, D. Kolousek, F. Kovanda, V. Dornicak, Water Air Soil Pollut. 149 (2003) 251.
[7] L.P. Cardoso, J. Tronto, E.L. Crepaldi, J.B. Valim, Mol. Cryst. Liq. Cryst. 390 (2003) 49.
[8] F. Li, Y. Wang, Q. Yang, D.G. Evans, C. Forano, X. Duan, J. Hazard. Mater. B125 (2005) 89.
[9] S. Miyata, Clays Clay Miner. 31 (1983) 305.
[10] L. Ingram, H.F.W. Taylor, Miner. Mag. 36 (1967) 465.
[11] R. Allmann, Acta Cryst. B24 (1968) 972.
[12] T. Kameda, F. Yabuuchi, T. Yoshioka, M. Uchida, A. Okuwaki, Water Res. 37 (2003) 1545.
[13] R.L. Frost, A.W. Musumeci, M.O. Adebajo, W. Martens, J. Therm. Anal. Calorim. 89 (2007) 95.
[14] S.J. Palmer, R.L. Frost, T. Nguyen, J. Therm. Anal. Calorim. 92 (2008) 879.
[15] H.J. Spratt, S.J. Palmer, R.L. Frost, Thermochim. Acta 479 (2008) 1.
[16] R.L. Frost, A. Soisnard, N. Voyer, S.J. Palmer, W.N. Martens, J. Raman Spectrosc. 40 (2009) 645.
[17] S.J. Palmer, A. Soisnard, R.L. Frost, J. Colloid Interface Sci. 329 (2009) 404.
[18] S.J. Palmer, H.J. Spratt, R.L. Frost, J. Therm. Anal. Calorim. 95 (2009) 123.
[19] S.J. Palmer, R.L. Frost, T. Nguyen, Coord. Chem. Rev. 253 (2009) 250.
[20] T. Kameda, T. Yoshioka, K. Watanabe, M. Uchida, A. Okuwaki, Appl. Clay Sci. 35 (2007) 173.
[21] J. Madarasz, P.P. Varga, G. Pokol, J. Anal. Appl. Pyrol. 79 (2007) 475.
[22] NIST Chemistry Webbook Standard Reference Database, No. 69, June 2005 Release. http://www.webbook.nist.gov/chemistry.
[23] M. Binnewies, E. Milke, Wiley-VCH Verlag GmbH, Thermochemical Data of Elements and Compound, 2nd edn. Weinheim, 2002.
[24] F.S. Chambers, T.K. Sherwood, Ind. Eng. Chem. 29 (1937) 1415.
[25] M.S. Peters, C.P. Ross, J.E. Klein, AIChE J. 1 (1955) 105.